

An Inkjet-Printed Solar-Powered Wireless Beacon on Paper for Identification and Wireless Power Transmission Applications

Sangkil Kim, *Student Member, IEEE*, Apostolos Georgiadis, *Senior Member, IEEE*, Ana Collado, *Member, IEEE*, and Manos M. Tentzeris, *Fellow, IEEE*

Abstract—This paper demonstrates the design of an 800-MHz solar-powered active wireless beacon composed of an antenna and an integrated oscillator on a low-cost paper substrate. Inkjet printing is used to fabricate the conductive circuit traces and the folded slot antenna, while the oscillator circuit is designed using off-the-shelf components mounted on the paper substrate. Flexible, low-cost, amorphous silicon (a-Si) solar cells are placed on top of the slot ground and provide autonomous operation of the active circuit eliminating the use of a battery. A prototype is built and characterized in terms of phase noise, radiation patterns, and the effect of solar irradiance. Such low-cost flexible circuits can find significant applications as beacon generator circuits for real-time identification and position purposes, wearable biomonitoring as well as solar-to-wireless power transfer topologies. The measured phase noise is -116 dBc/Hz at 1-MHz offset, while drain current is 4 mA and supply voltage is 1.8 V.

Index Terms—Active antennas, energy harvesting, flexible electronics, harmonic balance, inkjet printing, solar antenna, wireless beacon, wireless energy transfer, wireless identification.

I. INTRODUCTION

THE combination of sensor networks and RF identification (RFID) technologies have spurred numerous applications from logistics and Internet-of-things to monitoring and security, all of which require a capability for large-volume circuit production, as well as the use of low-cost fabrication methods on environmentally friendly flexible substrates, while energy autonomy is critical for operability in rugged environments [1]–[7].

As a result, implementations of flexible passive microwave circuit components, such as antennas, inductors, and transformers, utilizing substrates such as paper, polyethylene

terephthalate (PET), and textiles are receiving significant attention in the literature [2], [3]. The inkjet printing fabrication process, permitting a large-volume production and allowing a resolution below $50 \mu\text{m}$, has emerged as a popular alternative to traditional circuit board fabrication techniques, such as chemical etching and milling, finding increasing applicability in the electronics and sensors industries [1], [2].

The possibility of the inkjet printing of a complete system-on-substrate (SoS), based on multilayer flexible substrate modules and inkjet deposition of active devices remains a challenge, especially when it comes to operating at microwave frequencies. While inkjet printing of semiconducting polymers to develop organic thin-film transistors (OTFTs) [4] is still far from operation in the gigahertz frequency range, integration of off-the-shelf active electronic components onto flexible substrates provides an exciting alternative. The realization and integration of active topologies and sensors on flexible substrates, combined with passive interconnects, transmission lines, and antennas, presents a significant challenge with few notable examples in the literature, e.g., [1], [2] and [5]–[7], and presents the object of this study.

Furthermore, extending the operational autonomy of wireless sensors and transceivers has spurred significant efforts related to energy harvesting technologies, as well as wireless power transmission [8]. Toward this goal, the objective of this study is the integration of an active circuit with energy harvesting capability on a flexible low-cost paper substrate taking advantage of the capabilities of inkjet printing technology. For benchmarking proof-of-concept purposes, this paper demonstrates a prototype active antenna-based beacon operating at 800 MHz, transmitting power or sending identification information, which is powered by an amorphous silicon (a-Si) solar cell. Such circuits can be utilized as beacon signal generators in potential identification applications, or alternatively, as a solar-to-electromagnetic power converting circuit in wireless power transmission applications. The 800-MHz band is commonly utilized as the primary means of radio communication of data and voice for many city governments, especially for public safety and emergency. The operation frequency of the proposed active antenna can be easily scaled up or down to any other frequency band depending on the application.

The use of solar-based electromagnetic signal generation finds direct application in the field of wireless power transmission. Solar energy is captured using solar cells and used to bias a highly efficient oscillator element that will transmit

Manuscript received July 10, 2012; revised September 23, 2012; accepted September 24, 2012. Date of publication November 16, 2012; date of current version December 13, 2012. The work of S. Kim and M. M. Tentzeris was supported by SRC/IFC and NSF-ECS-0801798. The work of A. Georgiadis and A. Collado was supported by EU COST Action IC0803 (RFCSET) and EU Marie Curie Project FP7-PEOPLE-2009-IAPP 251557. This paper is an expanded paper from the IEEE MTT-S International Microwave Symposium, Montreal, QC, Canada, June 17–22, 2012.

S. Kim and M. M. Tentzeris are with the School of Electrical and Computer Engineering, Georgia Institute of Technology, Atlanta, GA 30308 USA (e-mail: ksangkil3@gatech.edu; etentze@ece.gatech.edu).

A. Georgiadis and A. Collado are with the Centre Tecnologic de Telecomunicacions de Catalunya, Castelldefels 08860, Spain (e-mail: ageorgiadis@cttc.es; acollado@cttc.es).

Color versions of one or more of the figures in this paper are available online at <http://ieeexplore.ieee.org>.

Digital Object Identifier 10.1109/TMTT.2012.2222922

its output signal through an antenna element. In order to take advantage of the area that the transmitting antenna elements occupy, the solar cells can be placed sharing the same area of the antenna or even on their ground plane. This way a compact structure that is capable of harvesting solar energy and then use it to transmit electromagnetic signals for wireless power transmission can be obtained. In [9], a solar powered active antenna on a nonflexible Arlon A25N substrate was presented, whereas in [10], a credit-card sized prototype solar powered active antenna on PET was demonstrated. This paper extends previous publications by additionally investigating the effect of solar irradiance on the active antenna performance, enabling the applicability of the proposed beacon to real-world scenarios. The active antenna oscillator is fabricated on a paper substrate with inkjet printing technology and the used solar cells are a-Si solar cells that are also flexible. The combination of paper substrate and flexible a-Si solar cells allow to have a conformal circuit that can be easily integrated in several application scenarios. Furthermore, this paper contains a detailed analysis of the electromagnetic, as well as the nonlinear circuit design, measurements of power gain radiation patterns of the active antenna, and characterization of the active antenna oscillator phase-noise performance.

In Sections II and III, design and simulation details of the passive and active antenna (beacon), respectively, are presented. Section IV contains measurements and characterization of the light-powered fabricated integrated prototypes.

II. PASSIVE ANTENNA DESIGN

Among the antenna requirements for low-power sensing and beacon applications are: 1) simple layout; 2) ease of integration with solar panels and active circuitry; 3) omnidirectional radiation; 4) frequency tuning capability or broadband performance; and 5) mechanical flexibility. The first requirement allows low-cost large-volume production required for RFID or wireless sensor network applications. Coplanar-waveguide (CPW) technology utilizes only one conductive layer, and therefore it is preferred to microstrip technology in terms of fabrication simplicity. Integration of solar panels with antennas allows for area reduction, and consequently, cost reduction. Slot antennas require a large ground plane, which is advantageous for solar cells, as well as additional circuitry integration. Frequency tuning or broadband characteristic is sought in order to easily reconfigure the antenna to cover different frequency bands depending on geographic location or specific applications. Mechanical flexibility is desired in order to easily place the antenna on different structures.

Taking into account the above requirements, a CPW slot antenna topology on a flexible paper substrate was selected. Specifically, a folded CPW slot structure was selected since it provides a greater flexibility to the designer to achieve the desired impedance over a wider frequency range compared to a single slot [11]. In a previous design [9], a grounded folded slot structure was used following [12], which allowed for a slight reduction in antenna size while somewhat reducing bandwidth and antenna efficiency. In this study, the shorting strip was not used, since size reduction was not a critical design goal,

and furthermore, the folded slot structure provided sufficient bandwidth.

The antenna is the output load of the oscillator, as well as a resonator effectively controlling the oscillation frequency. The broadband folded slot antenna configuration was chosen due to its stable input impedance throughout its operation frequency range, effectively facilitating the design of the oscillator and enhancing its stability. In addition, it is common in wireless modules operating in “rugged” environments that the antenna resonant frequency may shift because of the surrounding environment. The oscillator can be minimally affected by this phenomenon by using a broadband antenna with relatively small input impedance variability contrary to narrowband antennas, such as patch antennas. Additionally, the active antenna will be still able to operate even in the case that the oscillation frequency may vary. Therefore, the proposed active antenna can generate a “stable” power level regardless of the ambient environment, a critical feature in identification and power transmission applications.

A. Inkjet Printing and Paper Substrate

The RF properties of the paper substrate have been thoroughly investigated using the microstrip ring resonators method in [2]. The paper substrate is a very cheap, renewable, and biocompatible material. The dielectric constant (ϵ_r) of a 0.23-mm-thick Kodak photographic paper is 3.5 at 0.8–1.0 GHz, and the loss tangent ($\tan \delta$) is 0.07 through the frequency band of interest [2]. In addition, inkjet-printing technology has lots of advantages in the microwave area. It is a low-cost and an environmentally friendly fabrication process because it only drops the necessary conductive ink on the desired positions. It is different from conventional etching technology, which washes away the unwanted metal creating waste. In this way, circuits can be fabricated using only as much ink as it is required.

For the inkjet printing process, the Dimatix DMP2800 inkjet printer,¹ and the Dimatix 10 pL cartridge (DMC-11610) were utilized. The angle of the printer head was adjusted to achieve a print resolution of 1270 dots per inch (dpi). The ink that was used for the fabrication was Cabot CCI-300.² Once the desired pattern is inkjet printed, it needs to be cured in an oven for 4 h at 130 °C. The printed silver pattern usually has a dc conductivity in the range from 9×10^6 S/m to 1.1×10^7 S/m with a roughness of about 1 μm [13], [14].

The high loss tangent ($\tan \delta$) of paper is not important in the proposed design because the paper substrate is very thin (thickness of the paper = $6.1 \times 10^{-4} \lambda_0$). The magnetic field is generated along the slot and the electric field is built up across the narrow dimensions of the slot. However, the interaction of the electric field with the lossy paper substrate is very small, which results in low substrate loss. Therefore, the conductivity, thickness, and roughness of the metal is more important than the loss of substrate because those are critical factors of conductor loss. Therefore, the high loss of the paper substrate is not a critical design factor for the proposed design.

¹[Online]. Available: <http://www.dimatix.com/>

²[Online]. Available: <http://www.cabot-corp.com/New-Product-Development/Printed-Electronics/Products>



Fig. 1. Folded slot antenna geometry (gap of the CPW line: 0.2 mm).

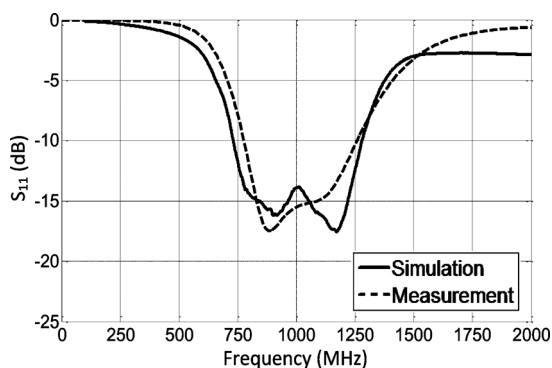


Fig. 2. Input S -parameters of the folded slot antenna.

B. Passive Antenna Design and Measurements

In Fig. 1, a photograph of the fabricated passive antenna prototype is presented with the corresponding dimensions. The slot length is 126 mm, and its width is 3.5 mm. The overall length of the antenna is 152 mm, width is 43.2 mm, and thickness of the paper substrate is $228.6 \mu\text{m}$. The antenna is fed by a CPW line with 5 mm of signal line width and 0.2 mm of ground-to-signal line gap.

A full-wave finite-element method (FEM) software tool (Ansys HFSS) is used to design and simulate the passive antenna. Simulated and measured results of the input S -parameters of the antenna are presented in Fig. 2, showing a good input impedance match over a bandwidth of approximately 41.5%. The simulated and measured radiation patterns of the antenna at 800 MHz are plotted in Fig. 3, showing a good agreement. The dashed lines in Fig. 3 shows radiation patterns of the passive antenna on the human body. It is noticeable that the gain of the passive antenna is decreased by about -10 dB when it is placed on the body, and an additional -10 dB of the antenna gain is decreased when a radiated wave passes through the human body. The antenna gains in free space and on the human body were evaluated in an outdoor setup and a value of approximately -6 dBi at 960 MHz was measured, as shown in Fig. 4. The gain of the antenna on the human body is about from -5 to -10 dB lower than that of the antenna in free space due to the effect of the lossy human body. The obtained low gain is mainly attributed to the limited dimensions of the ground plane. Fluctuations in the measured gain profile and variation with respect to the simulated values are attributed to the outdoor setup measurement error.

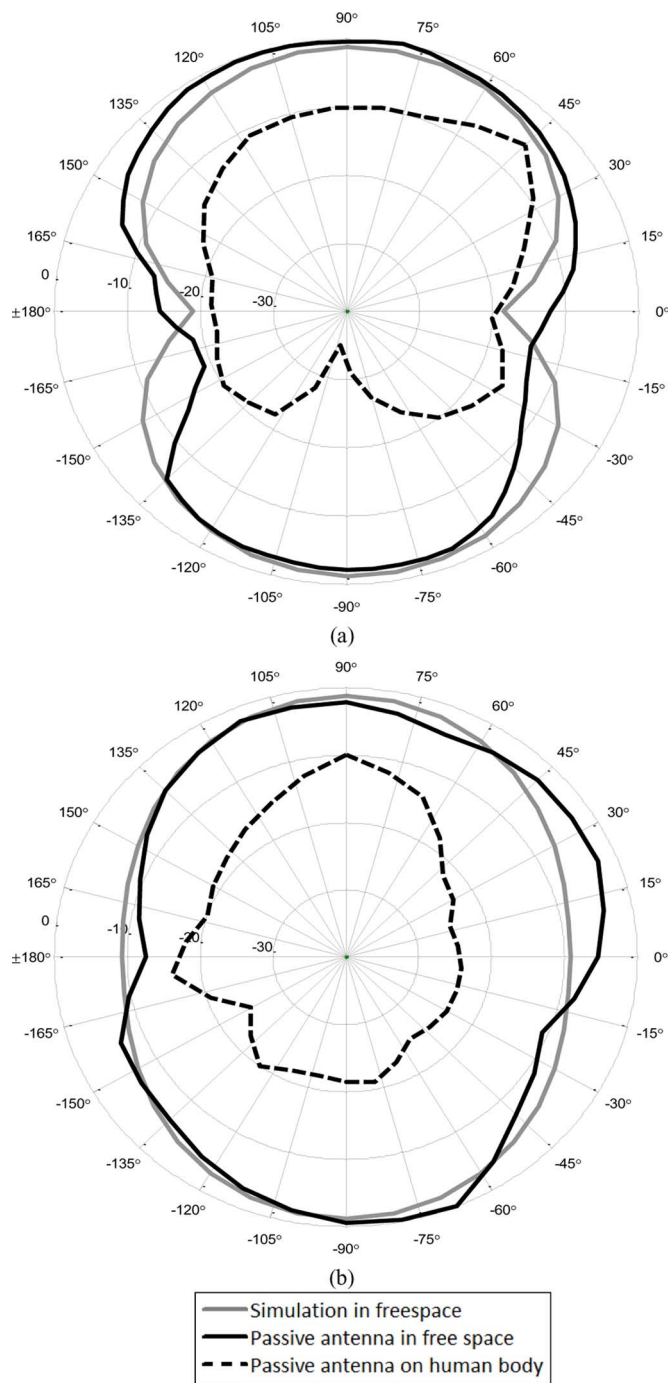


Fig. 3. Radiation patterns at 800 MHz. (a) E -plane. (b) H -plane.

III. ACTIVE ANTENNA OSCILLATOR DESIGN

An active oscillator antenna combines an oscillator circuit with a passive radiating structure [15]. It allows for a simple circuit layout, utilizing one active device and a minimum number of passive components, which can be integrated on the antenna structure—in this case, the ground plane surrounding the radiating slot, and thus, permitting a low-profile circuit design.

Diodes such as Gunn or impact ionization avalanche transit-time (IMPATT) diodes or transistors such as high electron-mobility transistors (HEMTs) or heterojunction bipolar transistors (HBTs) can be used as the active source for the

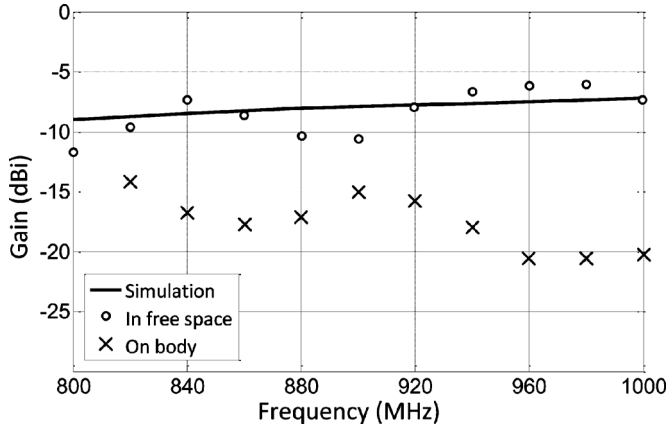


Fig. 4. Simulated and measured passive antenna gain.

oscillator. However, diodes are not suitable for identification and wireless power transmission applications due to their low dc-to-RF efficiency [15], [16]. On the other hand, transistors such as HEMT have high dc-to-RF efficiency, low heat dissipation, and low noise figure, which are critical factors in identification and wireless power transmission applications [15], [16]. In addition, transistors can be easily integrated with planar structures like slot or microstrip antennas [15], [16].

The oscillator circuit was designed using the NE3509M04 pseudomorphic HEMT (pHEMT). A one-stage reflection-type oscillator topology was selected with a simple passive LC tank (C_s and L_s). A multistage oscillator or an oscillator with a phase-locked loop (PLL) may increase the frequency stability of the active antenna oscillator; however, such designs lead to an increased circuit complexity and power consumption, which are undesired in beacon circuits for identification and wireless power transfer applications.

The circuit schematic of the designed oscillator is shown in Fig. 5. The antenna is connected to the gate terminal of the active device, while a source resistor R_1 is used to self-bias the device. Capacitors C_s , C_f , and C_d and inductors L_s and L_d tune the oscillation frequency around 800 MHz. Capacitor C_{d1} provides an RF short and isolates the dc feed from the oscillator circuit. The oscillator was initially designed without the solar cell power supply, using an operating dc power supply (HP/Agilent E3620A) voltage of 1.8 V, and drawing a current of 4 mA. A commercial harmonic-balance simulator (Agilent ADS) was used to simulate the oscillator circuit. A prototype oscillator was built and its performance characterized. The frequency of the oscillator is in good agreement with simulation within an expected yield variation of the off-the-shelf component values (Table I).

The oscillation frequency increases with the bias voltage, as shown in Fig. 6(a). Measurement of the oscillator frequency was made by capturing the radiated spectrum of the oscillator using a commercial broadband antenna and a spectrum analyzer. The frequency variation with the bias voltage can be utilized as a frequency-tuning mechanism, or alternatively, it can be minimized by placing a regulator circuit following the dc supply. The fabricated prototype frequency was less sensitive to bias voltage variation than in simulation. This difference can be attributed to yield variations of the used plane components

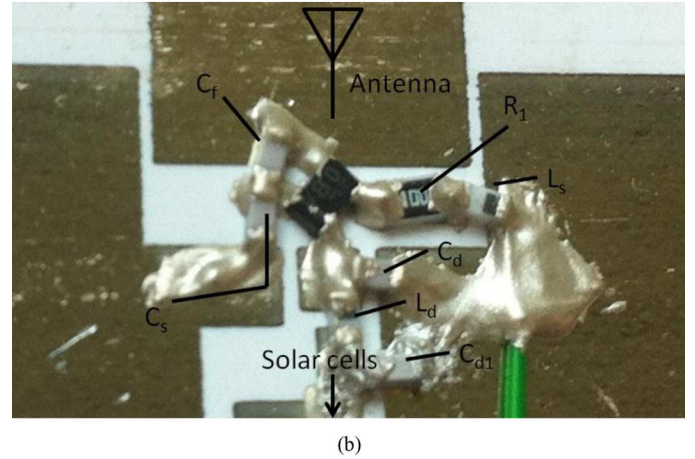
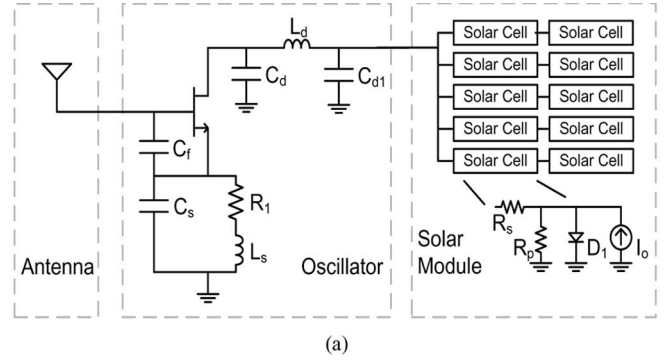


Fig. 5. Active oscillator antenna. (a) Circuit schematic. (b) Fabricated circuit.

TABLE I
CIRCUIT COMPONENT VALUES

Part	Value	Tolerance
C_d (pF)	1.5	± 0.1 pF
C_{d1} (μ F)	1.0	± 10 %
L_d (nH)	12.0	5 %
C_s (pF)	3.3	± 0.1 pF
C_f (pF)	3.3	± 0.1 pF
R_1 (Ohm)	10.0	5 %
L_s (nH)	18.0	5 %
f_{osc} (MHz)	~ 800	\square

and to associated layout parasitics not taken into account in the simulation stage. In addition, the discrepancy of simulation and measurement in Fig. 6(a) also resulted from imperfect modeling of active/passive device like a transistor, inductors, and capacitors. It is because additional parasitic effects such as capacitances and inductances from the surface mount components significantly effect the oscillation frequency of the circuit, and the comparatively low conductivity of inkjet-printed silver trace is also one of the most significant error source. Actual oscillation frequency is lower than the simulated value because the increased resistance and conductor loss cause an additional loading effect beside the unwanted parasitic effect of the transistor. The measured oscillator drain current was approximately 4 mA for bias voltages up to 4.0 V [see Fig. 6(b)]. Correspondingly, the dc power of the oscillator increases from 5.6

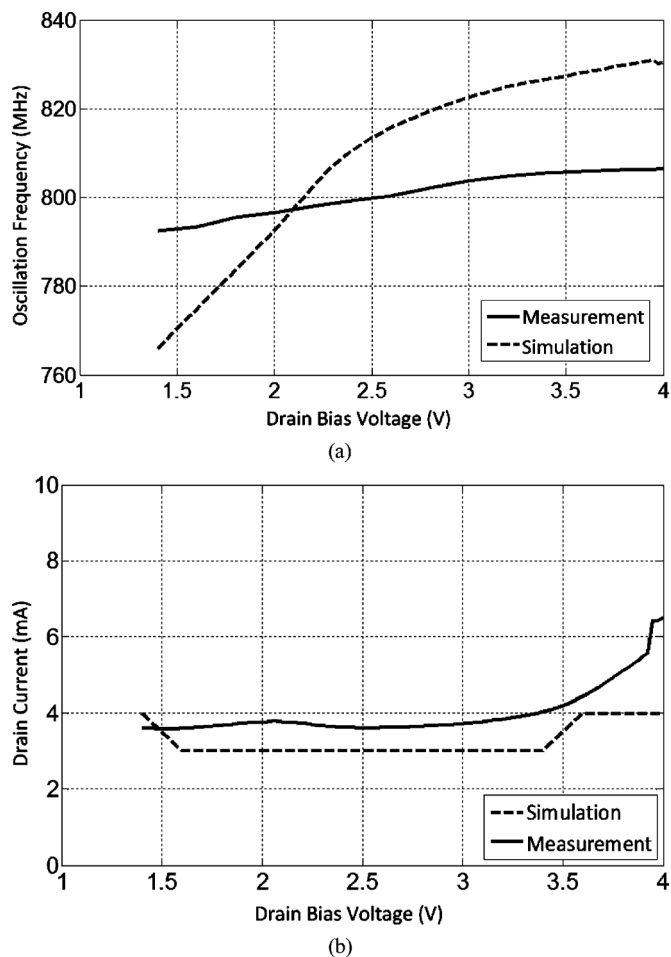


Fig. 6. Active oscillator antenna performance versus dc-bias voltage. (a) Oscillation frequency variation. (b) Current consumption variation.

to 16 mW as the supply voltage ranges from 1.4 to 4.0 V (Fig. 6). The voltage regulator dissipates power (P_D) about 1.2–8.8 mW as the supply voltage ranges from 2.1–4 V. Measured effective isotropic radiated power (EIRP) (dBm) patterns of the active antenna oscillator are shown in Fig. 7, showing a good agreement with the radiation patterns of the passive antenna as expected. The maximum EIRP on the E - and H -plane is 22.88 and 25.98 dBm, while the minimum EIRP on both planes is 3.91 and 20.34 dBm, respectively.

IV. AUTONOMOUS OPERATION USING SOLAR ENERGY

Autonomous operation of the active antenna was achieved by utilizing a-Si solar cells to harvest light energy, as shown in Fig. 8. One of the biggest challenges when integrating solar cells together with antenna elements is to select the optimum placement of the solar cell in order to not degrade the performance of the antenna. It is known in the literature that the solar cells have little effect on the radiation and input impedance characteristics of the antenna when properly placed, such as covering areas where the antenna field distribution is weaker [17]–[19]. Additionally, the solar cells should generate enough power to power the active antenna and the power provided should be stable in order to avoid variations in the oscillation frequency

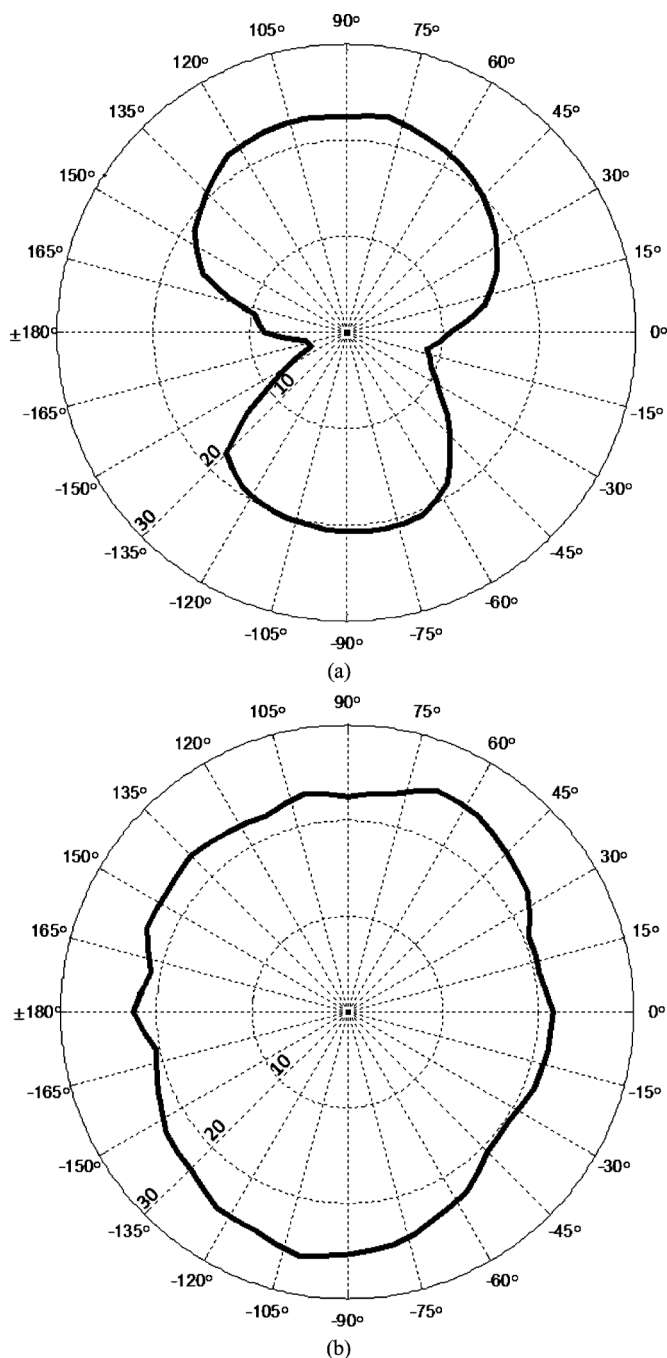


Fig. 7. Measured EIRP (dBm). (a) E -plane. (b) H -plane.

and also to generate a stable low phase-noise signal. The capacitor (C_{d1}) is mounted as shown in Fig. 5 to isolate the oscillator circuit from the dc feed and additionally the use of a voltage regulator at the output of the solar cell is considered in order to get a stable power from the solar cells, and consequently obtain a more stable oscillation frequency from the active antenna.

An amorphous silicon a-Si solar module (Power Film SP3-37) with a 4.1-V open-circuit voltage and 28-mA short-circuit current under 100 mW/cm² (1 sun: a unit of power flux from the sun) solar irradiation was used as a dc power supply. The SP3-37 module internally consists of five a-Si solar cells with approximately 0.85-V open-circuit voltage and 28-mA

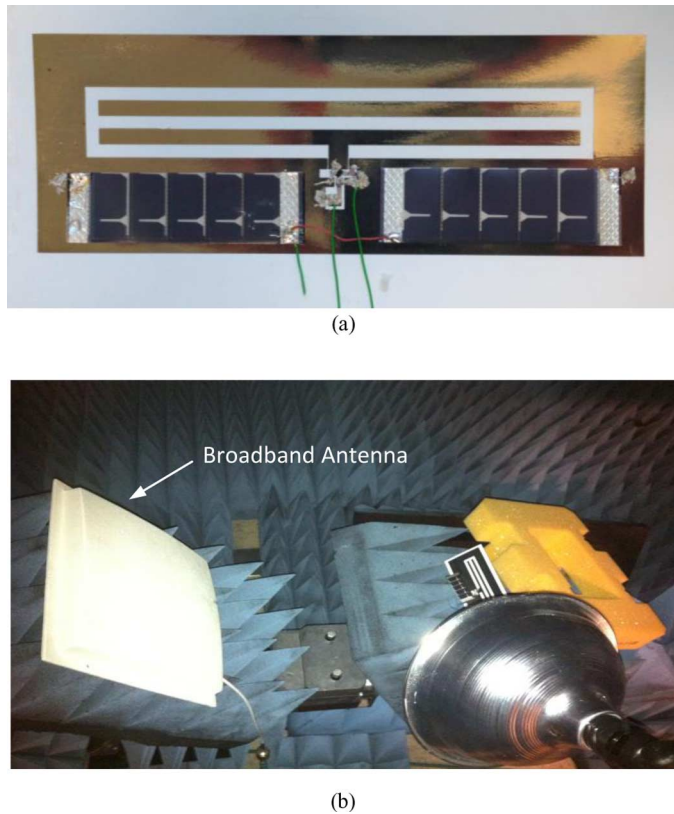


Fig. 8. Light powered active oscillator antenna. (a) Fabricated prototype. (b) Indoor measurement setup using a halogen lamp to illuminate the solar module.

short-circuit current in a series connection. In this study, one module was cut in two pieces across its long side and the two parts were properly placed on top of the active antenna ground plane and connected electrically in parallel [see Fig. 8(a)]. Each solar cell piece has approximately 4.1-V open-circuit voltage and 14-mA short-circuit current. An equivalent-circuit model of the solar cell consisting of an ideal current source, an ideal diode with saturation current I_s , a parallel resistance R_p , and a series resistance R_s was created in [8] by measuring the dc I - V curve of the cell. The equivalent-circuit model of the combined solar module is shown in Fig. 5, where the parameters of the solar cell model are $I_o = 1$ nA, $R_p = 110$ Ω , and $R_s = 7$ Ω [10].

The active beacon antenna was first characterized in an indoor environment by using a halogen lamp to excite the solar module. A luxometer was used to measure the illuminance at the active antenna position, while the distance of the halogen lamp was varied. Illuminance is typically used to characterize luminous sources at indoor environments. It is a photometric measure, which corresponds to the irradiance weighted by a luminosity function corresponding to the sensitivity of the human eye to light [19]. Solar irradiance of 100 mW/cm² (1 sun) corresponds to 100 klux illuminance [19]. The measured illuminance at the solar cell location is about 1.8×10^5 lux, 6×10^4 lux, and 2×10^4 lux when its distance from the halogen lamp is 127, 300, and 500 mm, respectively. The solar cell's short-circuit current (I_{sc}) and open-circuit voltage (V_{oc}) depending on illuminance are shown in Fig. 9. It shows that the oscillation

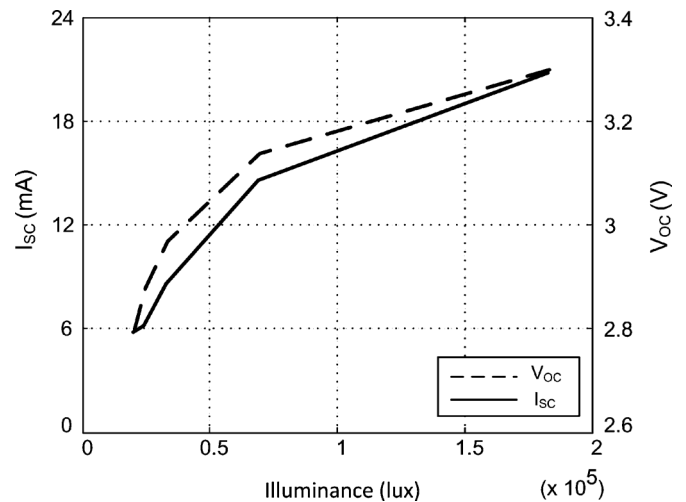


Fig. 9. Solar cell I_{sc} (short-circuit current) and V_{oc} (open-circuit voltage) versus illuminance.

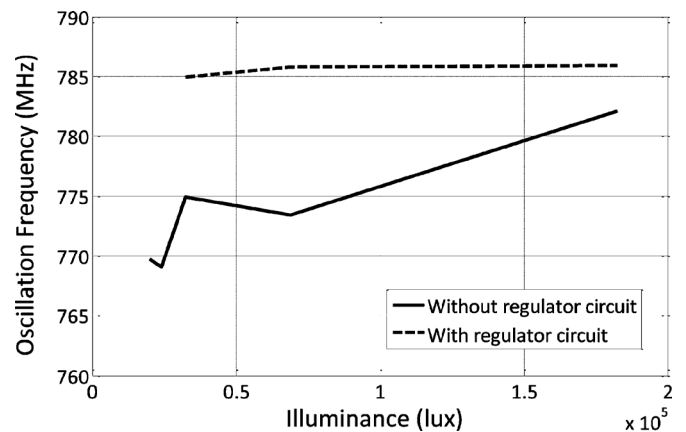


Fig. 10. Oscillation frequency versus illuminance with and without regulator circuit.

frequency can be stabilized by introducing a voltage regulator circuit since it supplies stable dc power to the oscillator. The stable oscillation frequency results in ease of matching between the antenna and oscillator output, as well as due to the broadband property of the antenna. Figs. 6, 9, and 10 show that the oscillation frequency can be stabilized when the illuminance is higher than 3.3×10^5 lux since the solar cell is able to produce enough power to operate the circuit. The solar cell generates 16.2–28.6 mW depending on illuminance, but the active antenna requires 6–28 mW, which is affordable power from the solar cell providing the illuminance is higher than 3.26×10^4 lux. The variation of the oscillator frequency with the illuminance is shown in Fig. 10. For illuminance values less than 2×10^4 lux, it was not possible to power up the oscillator. The frequency of oscillation is reduced compared to Fig. 6 due to the loading effect of the solar modules.

The observed frequency variation is also due to the measurement setup as the lamp structure includes a metallic reflector [see Fig. 8(b)] that is affecting the antenna impedance, and subsequently the oscillator frequency. A commercial regulator LT1763-1.8 with 1.8-V output voltage by Linear Technology, Milpitas, CA, was additionally used to minimize the dc

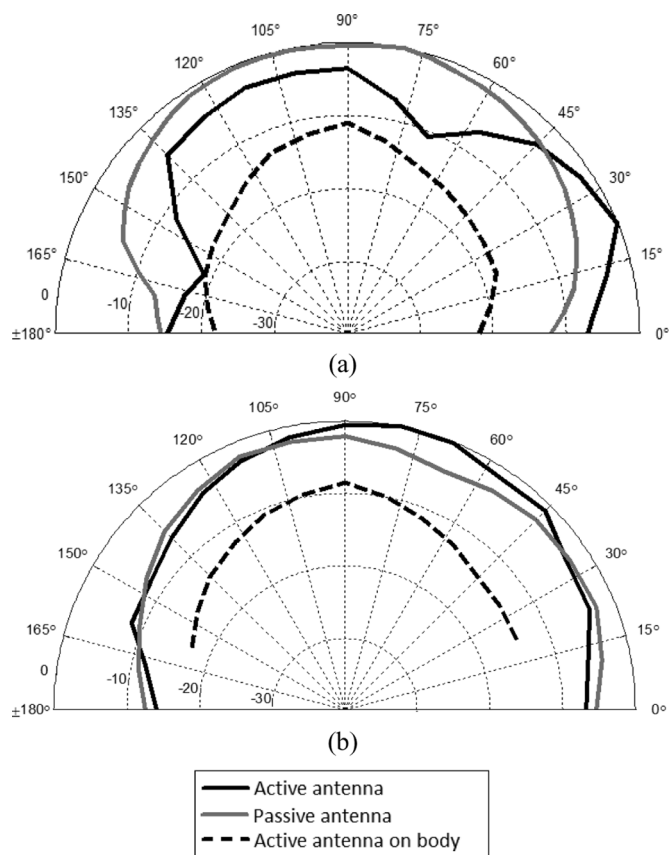


Fig. 11. Radiation patterns of active antenna oscillator under sun light conditions. (a) E -plane. (b) H -plane.

supply variation due to the illuminance variation. The dissipated power (P_D) of the regulator is in the range of 4.05–6.05 mW, including quiescent power (P_Q) when it is powered by the solar cell providing the illuminance is stronger than 3.26×10^4 lux. Measurements are included in Fig. 10, demonstrating a significantly reduced frequency dependence on the illuminance. It was not possible to properly power the regulator for illuminance values less than 3.26×10^4 lux. Finally, a slight increase of the oscillating frequency was observed when using the regulator. This is also attributed to the loading effect of the regulator on the active circuit.

Radiation patterns of the solar powered active antenna were obtained outdoors at the Georgia Institute of Technology, Atlanta, for a measured illuminance of 1.6×10^5 lux. The radiated power from the solar-powered active antenna with the regulator circuit is measured, and the measured power patterns are shown in Fig. 11. In order to test the effect of the flexing of the paper substrate on the radiation performance of the autonomous beacon, H -plane on-body measurements were also performed by placing the antenna on top of a cotton shirt and at the chest of a person showing an approximately 10-dB reduction in antenna gain (Fig. 11). Similar omnidirectional radiation patterns in free space in Fig. 11 suggest noteworthy results that the solar-powered active antenna has similar radiation patterns to that of the passive antenna. In addition, it loses omnidirectionality when the active antenna is mounted in the human body due to power absorption of the human body since a human body is a very lossy and high dielectric material.

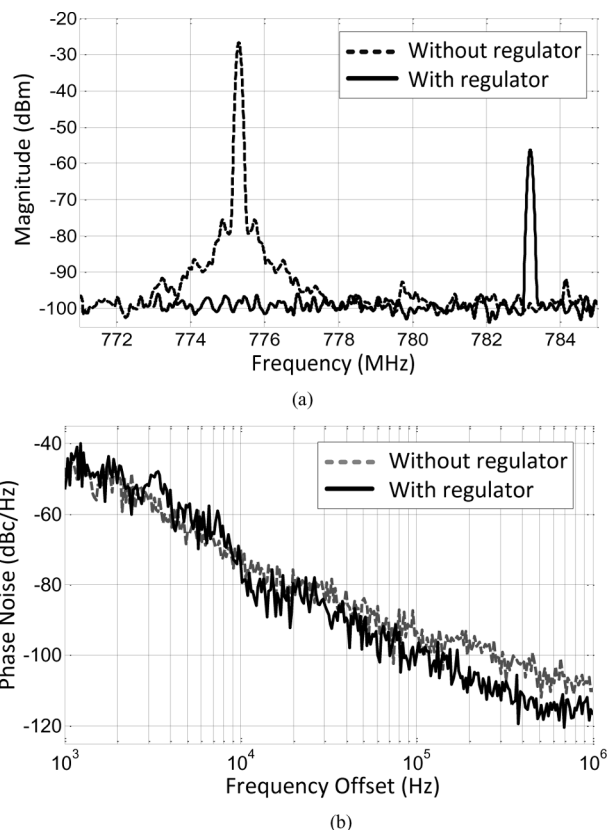


Fig. 12. Measured: (a) power spectra and (b) phase noise of active antenna under sun light conditions without/with regulator circuit.

Finally, the power spectrum and the phase noise of the solar powered active antenna was measured. The dashed line in Fig. 12(a) shows the power spectrum of the antenna powered by solar cell without the voltage regulator circuit, while the solid line shows the spectrum of the solar-powered active antenna with the regulator circuit in outdoor environment. It should be noted that solar illuminance with the voltage regulator leads to a cleaner spectrum than the one obtained without the regulator circuit. It is because output voltage of the solar cell is fluctuating depending on an illuminance of the sun. The magnitude difference of the spectra is due to measurement error. The commercial broadband antenna, which have been shown in Fig. 8, cannot be used to get the power spectrum in the outdoor environment because it captures unwanted noises such as TV or other wireless signals too. An open coaxial cable was placed near the antenna to catch a signal from the antenna, which resulted in a magnitude difference of the spectra. The observed frequency shifting of the antenna when it is connected to the regulator is due to loading effect of the regulator circuit, which includes capacitors and the regulator chip.

The dashed line in Fig. 12(b) shows the phase noise of the antenna for an illuminance of 1.6×10^5 lux without the regulator, while the solid line in Fig. 12(b) shows the same measurement by including the regulator circuit. A phase noise value of -116.6 dBc/Hz at 1-MHz offset was measured for the circuit that includes the voltage regulator, showing an improvement in the phase noise of around 5 dB due to the better frequency stability when using the voltage regulator. The phase noise of the antenna with the regulator is slightly higher than that of the

antenna without the regulator at the frequency offset band of 3–4 kHz. It can be considered as an measurement error. This error can be caused due to fluctuation of intensity of sunlight and interference of unwanted signal since the measurement took place in an outdoor environment.

V. CONCLUSION AND FUTURE WORK

The fabrication of flexible autonomous sunlight-powered batteryless active beacons on low-cost paper substrates using inkjet printing technology has been demonstrated. An 800-MHz RF prototype integrating an inkjet-printed folded slot antenna and an oscillator with solar cells on paper has verified the unique capabilities of this approach, potentially paving the way for scalable conformal low-cost wireless identification circuits and efficient wireless power transfer topologies. A future challenge toward enabling complete system integration consists of inkjet printing of thin-film energy storage elements such as capacitors and batteries.

The next step of this study is to perform an optimized design of the oscillator element in order to maximize its dc-to-RF conversion efficiency by considering class-E topologies for the oscillator element. As one of the targeted applications of the proposed system is wireless power transmission, maximizing the dc to RF efficiency in the oscillator will also maximize the amount of RF power that the system will transmit. In addition, this type of system could be potentially used to increase the range of passive RFIDs. In [20], a similar system was used to increase the range of a passive RFID by, instead of transmitting the signal out of the oscillator, directly feeding it into the RFID. The proposed topology showed an increase in the reading range of the RFID. Based on the same idea as in [20], another potential application is to use the system presented in this paper to transmit RF signals in an RFID environment. The presence of additional RF signals apart from the signals from the reader has shown improvement in the reading range of passive RFIDs.

REFERENCES

- [1] R. Vyas, V. Lakafosis, H. Lee, G. Shaker, L. Yang, G. Orecchini, A. Traillie, M. M. Tentzeris, and L. Roselli, "Inkjet printed, self-powered, wireless sensors for environmental, gas, and authentication-based sensing," *IEEE Sens. J.*, vol. 11, no. 12, pp. 3139–3152, Dec. 2011.
- [2] L. Yang, A. Rida, R. Vyas, and M. M. Tentzeris, "RFID tag and RF structures on a paper substrate using inkjet-printing technology," *IEEE Trans. Microw. Theory Tech.*, vol. 55, no. 12, pp. 2894–2901, Dec. 2007.
- [3] A. Tronquo, H. Rogier, C. Hertleer, and L. Van Langenhove, "Robust planar textile antenna for wireless body LANs operating in 2.45 GHz ISM band," *Electron. Lett.*, vol. 42, no. 3, pp. 142–143, Feb. 2006.
- [4] L. Basiricò, P. Cosseddu, B. Fraboni, and A. Bonfiglio, "Inkjet printing of transparent, flexible, organic transistors," *Thin Solid Films*, vol. 520, no. 4, pp. 1291–1294, Dec. 2011.
- [5] A. Rida, L. Yang, R. Vyas, and M. M. Tentzeris, "Conductive inkjet-printed antennas on flexible low-cost paper-based substrates for RFID and WSN applications," *IEEE Antennas Propag. Mag.*, vol. 51, no. 3, pp. 13–23, Jun. 2009.
- [6] B. S. Cook and A. Shamim, "Inkjet printing of novel wideband and high gain antennas on low-cost paper substrate," *IEEE Trans. Antennas Propag.*, vol. 60, no. 9, pp. 4148–4156, Sep. 2012.
- [7] B. Ando and S. Baglio, "Inkjet-printed sensors: A useful approach for low cost, rapid prototyping," *IEEE Instrum. Meas. Mag.*, vol. 14, no. 5, pp. 36–40, Oct. 2011.
- [8] N. Shinohara, "Power without wires," *IEEE Microw. Mag.*, vol. 12, no. 7, pp. S64–S73, Dec. 2011.
- [9] F. Giuppi, A. Georgiadis, S. Via, A. Collado, R. Vyas, M. M. Tentzeris, and M. Bozzi, "A 927 MHz solar powered active antenna oscillator beacon signal generator," in *Proc. IEEE Top. Wireless Sensors and Sensor Networks Conf.*, Santa Clara, CA, Jan. 15–18, 2012, pp. 1–4.

- [10] A. Georgiadis, A. Collado, S. Kim, H. Lee, and M. M. Tentzeris, "UHF solar powered active oscillator antenna on low cost flexible substrate for application in wireless identification," in *IEEE MTT-S Int. Microw. Symp. Dig.*, Montreal, QC, Canada, Jun. 17–22, 2012, pp. 1–3.
- [11] H.-S. Tsai and R. A. York, "FDTD analysis of CPW fed folded-slot and multiple-slot antennas on thin substrates," *IEEE Trans. Antennas Propag.*, vol. 44, no. 2, pp. 217–226, Feb. 1996.
- [12] R. B. Waterhouse and D. Novak, "Small folded CPW fed slot antennas," in *Proc. IEEE Antennas Propag. Soc. Int. Symp.*, Jul. 9–14, 2006, pp. 2599–2602.
- [13] S. Kim, Y.-J. Ren, H. Lee, A. Rida, S. Nikolaou, and M. M. Tentzeris, "Monopole antenna with inkjet-printed EBG array on paper substrate for wearable applications," *IEEE Antennas Wireless Propag. Lett.*, vol. 11, no. , pp. 663–666, 2012.
- [14] M. L. Allen, M. Aronniemi, T. Mattila, A. Alastalo, K. Ojanpera, M. Suhonen, and H. Seppa, "Electrical sintering of nanoparticle structures," *Nanotechnology*, vol. 19, 2008, Art. ID 175201.
- [15] K. Chang, R. A. York, P. S. Hall, and T. Itoh, "Active integrated antennas," *IEEE Trans. Microw. Theory Tech.*, vol. 50, no. 3, pp. 937–944, Mar. 2002.
- [16] H. C. Yen, R. Esfandiari, Y. Hwang, K. Tan, C. Liu, M. Aust, R. Carandang, and H. Wang, "A monolithic approach for Q-band integrated active phased array transmitting antenna," in *IEEE Antennas Propag. Soc. Int. Symp.*, Jul. 1992, vol. 1, pp. 126–129.
- [17] M. Tanaka, Y. Suzuki, K. Araki, and R. Suzuki, "Microstrip antennas with solar cells for microsattellites," *Electron. Lett.*, vol. 31, pp. 263–266, 1996.
- [18] S. Vaccaro, J. R. Mosig, and P. de Maagt, "Two advanced solar antenna "SOLANT" designs for satellite and terrestrial communications," *IEEE Trans. Antennas Propag.*, vol. 51, no. 8, pp. 2028–2034, Aug. 2003.
- [19] A. Virtuani, E. Lotter, and M. Powalla, "Influence of the light source on the low-irradiance performance of Cu(In,Ga)Se₂ solar cells," *Solar Energy Mater. Solar Cells*, vol. 90, no. 14, pp. 2141–2149, Sep. 2006.
- [20] A. Georgiadis and A. Collado, "Improving range of passive RFID tags utilizing energy harvesting and high efficiency class-e oscillators," in *2012 6th Eur. Antennas Propag. Conf.*, Mar. 26–30, 2012, pp. 3455–3458.



Sangkil Kim (S'12) received the B.S. degree in electrical and electronic engineering from Yonsei University, Seoul, Korea, in 2010, the M.S. degree in electrical engineering from the Georgia Institute of Technology, Atlanta, in 2012, and is currently working toward the Ph.D. degree at the Georgia Institute of Technology.

He is currently involved with the design and fabrication of novel wearable electronics for body area networks.



Apostolos Georgiadis (S'94–M'03–SM'08) was born in Thessaloniki, Greece. He received the B.S. degree in physics and M.S. degree in telecommunications from the Aristotle University of Thessaloniki, Thessaloniki, Greece, in 1993 and 1996, respectively, and the Ph.D. degree in electrical engineering from the University of Massachusetts at Amherst, in 2002.

In 2002, he joined Global Communications Devices (GCD), North Andover MA, as a Systems Engineer, involved with CMOS transceivers for wireless network applications. In June 2003, he joined Bernai Inc., Minnetonka, MN, as an RF/Analog Systems Architect. In 2005, he joined the University of Cantabria, Santander, Spain, as a Juan de la Cierva Fellow Researcher. In March 2007, he joined the Centre Tecnologic de Telecomunicacions de Catalunya (CTTC), Castelldefels, Spain, as a Senior Research Associate in the area of communications subsystems. He serves on the Editorial Board of the *Radioengineering Journal*. His research interests include energy harvesting, RFID technology, nonlinear microwave circuit design, active antenna arrays, and specifically coupled oscillator arrays.

Dr. Georgiadis is the chairman of COST Action IC0803 RF/microwave communication subsystems for emerging wireless technologies (RFCSET). He is the coordinator of Marie Curie Industry–Academia Pathways and Partnerships (IAPP) project Symbiotic Wireless Autonomous Powered System (SWAP). He is a member of the IEEE MTT-S TC-24 RFID Technologies and IEEE MTT-S TC-26 Wireless Energy Transfer and Conversion.



Ana Collado (M'07) was born in Santander, Spain. She received the B.S. degree in telecommunications engineering and Ph.D. degree from the University of Cantabria, Santander, Spain, in 2002 and 2007, respectively.

In 2002, she was with the University of the Basque Country, Bilbao, Spain, where she was involved in the study of the uncertainty in noise-figure measurements in monolithic-microwave integrated-circuit low-noise amplifiers. Since July 2007, she has been a Research Associate with the Centre Tecnològic de Telecomunicacions de Catalunya, Castelldefels, Spain, where she is involved in the area of communication subsystems. Her areas of interest include the development of techniques for practical bifurcation control and stability analysis of power amplifiers and coupled oscillator systems, RFID technology, energy harvesting, and wireless power transmission solutions.

Dr. Collado was a 2011 Marie Curie Fellow Researcher for Project EU FP7-251557 Symbiotic Wireless Autonomous Powered system (SWAP), and Management Committee Member and Grant Holder Representative of EU COST Action IC0803, RF/microwave communication subsystems for emerging wireless technologies (RFCSET).



Manos M. Tentzeris (S'89–M'92–SM'03–F'10) received the Diploma degree in electrical and computer engineering (*magna cum laude*) from the National Technical University of Athens, Athens, Greece, and the M.S. and Ph.D. degrees in electrical engineering and computer science from The University of Michigan at Ann Arbor.

He is currently a Professor with School of Electrical and Computer Engineering, Georgia Institute of Technology, Atlanta. He has helped develop academic programs in highly integrated/multilayer packaging for RF and wireless applications using ceramic and organic flexible materials, paper-based RFIDs and sensors, biosensors, wearable electronics, inkjet-printed electronics, "Green" electronics and power scavenging, nanotechnology applications in RF, microwave microelectromechanical systems (MEMs), system-on-package (SOP)-integrated (ultra-wideband (UWB), multiband, millimeter wave, conformal) antennas and adaptive numerical electromagnetics (FDTD, multiresolution algorithms). He heads the ATHENA research group (20 researchers). He is currently the head of the Electromagnetics Technical Interest Group, School of Electrical and Computer Engineering, Georgia Institute of Technology. From 2006 to 2010, he was the Georgia Electronic Design Center Associate Director for RFID/sensors

research. From 2003 to 2006, he was the Georgia Institute of Technology National Science Foundation (NSF) Packaging Research Center Associate Director for RF Research and the RF Alliance Leader. During the summer of 2002, he was a Visiting Professor with the Technical University of Munich, Munich, Germany. During the summer of 2009, he was a Visiting Professor with GTRI-Ireland, Athlone, Ireland. In the summer of 2010, he was a Visiting Professor with LAAS-CNRS, Toulouse, France. He has authored or coauthored over 420 papers in refereed journals and conference proceedings, five books, and 19 book chapters. He is an Associate Editor for the *International Journal on Antennas and Propagation*.

Dr. Tentzeris was the Technical Program Committee (TPC) chair for the 2008 IEEE Microwave Theory and Techniques Society (IEEE MTT-S) International Microwave Symposium (IMS) and the chair of the 2005 IEEE CEM-TD Workshop. He is the vice-chair of the RF Technical Committee (TC16), IEEE CPMT Society. He is the founder and chair of the RFID Technical Committee (TC24), IEEE MTT-S. He is the secretary/treasurer of the IEEE C-RFID. He is a member of URSI-Commission D and the MTT-15 committee. He is an Associate Member of the European Microwave Association (EuMA). He is a Fellow of the Electromagnetic Academy. He is a member of the Technical Chamber of Greece. He is an IEEE MTT-S Distinguished Microwave Lecturers (2010–2012). He was an associate editor for the IEEE TRANSACTIONS ON MICROWAVE THEORY AND TECHNIQUES. He is an associate editor for the IEEE TRANSACTIONS ON ADVANCED PACKAGING. He has given over 100 invited talks to various universities and companies all over the world. He was the recipient/corecipient of the 2012 FiDiPro Professorship in Finland, the 2010 IEEE Antennas and Propagation Society Piergiorgio L. E. Uslenghi Letters Prize Paper Award, the 2011 International Workshop on Structural Health Monitoring Best Student Paper Award, the 2010 Georgia Institute of Technology Senior Faculty Outstanding Undergraduate Research Mentor Award, the 2009 IEEE TRANSACTIONS ON COMPONENTS AND PACKAGING TECHNOLOGIES Best Paper Award, the 2009 E. T. S. Walton Award of the Irish Science Foundation, the 2007 IEEE Antennas and Propagation Society (AP-S) Symposium Best Student Paper Award, the 2007 IEEE MTT-S IMS Third Best Student Paper Award, the 2007 ISAP 2007 Poster Presentation Award, the 2006 IEEE MTT-S Outstanding Young Engineer Award, the 2006 Asian-Pacific Microwave Conference Award, the 2004 IEEE TRANSACTIONS ON ADVANCED PACKAGING Commendable Paper Award, the 2003 NASA Godfrey "Art" Anzic Collaborative Distinguished Publication Award, the 2003 IBC International Educator of the Year Award, the 2003 IEEE CPMT Outstanding Young Engineer Award, the 2002 International Conference on Microwave and Millimeter-Wave Technology Best Paper Award, the 2002 Georgia Institute of Technology-Electrical and Computer Engineering Outstanding Junior Faculty Award, the 2001 ACES Conference Best Paper Award, the 2000 National Science Foundation (NSF) CAREER Award, and the 1997 Best Paper Award of the International Hybrid Microelectronics and Packaging Society.